Proceedings of the 9th International Conference on Aluminium Alloys (2004)
Edited by J.F. Nie, A.J. Morton and B.C. Muddle

A Monte Carlo Simulation on PFZ Formation in a Model Binary Alloy

H.Okuda and S.Ochiai

International Innovation Center, Kyoto University, Sakyo-ku Kyoto 606-8501 Japan

Keywords: Monte Carlo Simulation, Kinetic Ising Model, Precipitation Free Zone, Size Distribution

Abstract

Monte Carlo simulations using kinetic Ising model and semi GC boundary conditions have been performed on a fcc model binary alloy. The effects of the solute depletion owing to the grain boundary precipitation and the vacancy depletion owing to the annihilation of quenched–in vacancies were taken into account. The characteristic microstructures for both effects were examined in detail from both kinetic and microstructural points of view, using distribution of the precipitates. The vacancy depletion scheme gave a retarded kinetics near the grain boundary, which suggests a gradual size change in space near the grain boundary.

1. Introduction

Grain boundary precipitation and vacancy depletion are the two most important factors that determines the formation of precipitation-free zone (PFZ). Preceding experimental works [1-5] showed that either the depletion of solute atoms near the grain boundary due to more stable grain boundary precipitation, or the vacancy depletion due to annihilation of excess vacancy at the grain boundary during quench, plays important role during the aging process, depending on the quenching and aging conditions. In the recent development of precipitation strengthened Al alloys, it is becoming more and more important to control the PFZ microstructure to obtain better performance that is expected for well-controlled microstructure inside the grains. Experimentally, we can not control the solute depletion and vacancy depletion independently, since both of them occur to some extent during quenching, and should be strongly affected by the microstructure of grain boundary. Therefore, a computer simulation is a useful tool to have a insight into the effect of each depletion on the microstructures and their development. Since the kinetics of PFZ growth under solute depletion condition are reported to be similar for the case where the precipitates have different crystal structure and for the case where the case that the lattice point is conserved[1,3-5], we may use a rigid lattice model system to examine a characteristic microstructure during heat treatment. In the present simulation, we examined the effect of solute depletion and vacancy depletion separately for large supersaturation case, and show that the mechanism and kinetics of the precipitation process that occurs under the two depletion that lead to PFZ is quite different.

2. Simulation Procedure

In the present simulation, we adopted a Monte Carlo simulation utilizing Kawasaki Dynamics[6]. In order to describe the solute depletion, we adopted a boundary condition that a mass reservoir is attached to the grain boundary, whose concentration is given externally from the equilibrium condition for the grain boundary precipitation.

In the present simulation, we adopted a rigid fcc lattice without lattice distortion, and the internal energy was simply calculated by the nearest neighbor pair interaction energy. Since we are simulating the phase separation system, the exchange integral, or the interaction parameter is a positive constant.

This assumption leads to a well-defined phase diagram, whose relationship between the interaction parameter, Ω, and the critical temperature, Tc, of the phase diagram is given by

$$\Omega / R\,Tc = 2.450. \qquad (1)$$

where R : the gas constant and T : the temperature. The system size is 60 x 60 x 300 unit cells, with the long size perpendicular to the grain boundary. The grain boundary is placed at z=0, and has a direct contact with the mass reservoir as shown in Figure. 1. The concentration of the mass reservoir is kept constant, $c = c_B$, during annealing. For the solute depletion case, c_B is lower than that of the equilibrium concentration of the phase boundary inside the grain. For vacancy depletion case, we set the boundary condition of the solute concentration at z=0 as the same one as that for z=300. A periodic boundary condition is used for x and y direction, and at z=300, i.e., at the innermost place inside the grain, we assume that the concentration gradient vanishes.

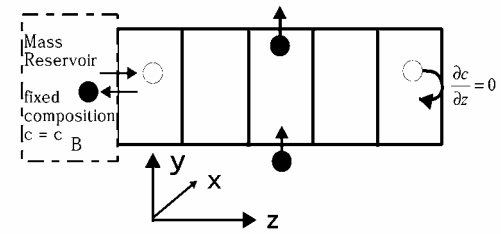

Figure 1: Schematic explanation of the boundary conditions and initial condition in the present simulation. The grain boundary precipitation is expressed in terms of mass absorption into a mass reservoir placed at the grain boundary.

The initial composition used in the present simulation was mainly 0.07, and 0.04 was also used to examine the effect of smaller supersaturation. The heat treatment procedure is illustrated in Figure. 2.

The system was first solution-treated at 1.0Tc, and aged at 0.55 Tc. The aging temperature of 0.55Tc corresponds to the temperature around T6 treatment.

After aging treatment, some of the simulations made an additional ‘up quench’ or reversion treatment, to see the effect of partial dissolution during second aging. The vacancy depletion was assumed to be made during quenching, so that we have a concentration gradient of vacancy during the quench.

Since we can assume that vacancy may behave as nearly ideal solution at high temperature with small concentration, we described the vacancy concentration profile at the as-quenched state by a error function, whose characteristic diffusion length is given as an initial condition.

For the solute depletion model, we need to give the solute concentration at the grain boundary, c_B, separately, to model the situation that c_B corresponds to the solubility limit for stable phase at grain boundaries. From separate Monte Carlo simulations, the solubility limit inside the grain was evaluated to be 0.019 +/- 0.002 at T=0.55Tc.

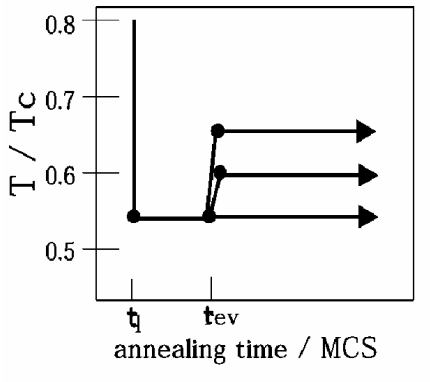

Figure 2: Heat treatment used in the present simulation. A short solution treatment at 1.0Tc was made to set up the initial condition, and then aging treatment with solute or vacancy depletion was made at 0.55Tc. The concentration of the mass reservoir, c_B, was kept constant during aging.

Since the ratio of the solubility limit for stable precipitates to that for metastable precipitates lies between 0.3 and 0.7 for age-hardenable Al alloys, we chose c_B=0.01.

The microstructure and the temporal evolution of the system should be characterized by the cluster size and its distribution. When a system with simple periodic boundary condition was aged in a two-phase region, it is well known that the average cluster size increase monotonically and homogeneously with time[7-8]. In the present simulation, the size of the cluster was evaluated by two approaches. One is the average cluster size calculated from Warren-Cowley short range order (SRO) parameters, defined by [9],

$$\alpha(n) = 1 - p_A(n)/c_A = 1 - p_B(n)/c_B \qquad (2)$$

with (n) means the n th neighbor from the origin, and $P_i(n)$ the probability of finding i (i=A or B) atom in the n th neighbor of the other (B or A) atom, and the probability is averaged over the sample volume of interest. The SRO is proportional to the concentration-concentration correlation function of the solute atoms, $\gamma(r)$ [10], defined by ;

$$\gamma(r) = \int \{c(r') - c_0\}\{c(r+r') - c_0\} dr' \,. \qquad (3)$$

Since the correlation function for a spherical precipitate is given by

$$\gamma(r) = v\Delta c^2 \left[1 - 3r/4R + r^3/16R^3\right] \qquad (4)$$

we can obtain the average size of clusters, R, by plotting the SRO as a function of distance between the origin and the n th neighbor site, r(n).

The other approach is a direct calculation of topological connection of solute atoms to identify individual cluster. The average structure is useful to interpret the microstructural evolution from thermodynamical viewpoint, whereas the latter case is useful to examine spatially heterogeneous microstructure such as the microstructure of PFZ front.

3. Results and Discussions

3.1 Solute Depletion Case

Figure 3 shows the change in the average concentration as a function of the distance from grain boundary, z, with aging time at 0.55Tc, when the solute concentration at the boundary, c_B is fixed at 0.01. The profile is averaged over 60 x60 unit cells in x-y plane and also over 7 independent runs. During solution treatment, there is no inhomogeneity in the concentration throughout the system. After quenching and simultaneous aging inside the

grain and the grain boundary precipitation, it is clearly seen that the average concentration near the grain boundary start to decrease. After t=926 Monte Carlo Steps (MCS), the profile exhibits three distinct regions[11].

The first one is the PFZ region, the second one is a transient region, and the third one is the bulk region where the concentration remains the same as the initial composition. At the PFZ region, the concentration changes from c_B at the grain boundary (z=0) to about 0.02 at the PFZ/Transient region boundary, at t=6940 MCS. Recalling that the solubility limit of the system at T=0.55Tc is 0.019, the PFZ region is characterized by the single phase diffusion field where the solute atoms flow towards the grain boundary within the solid-solution state. In contrast, the transient and the bulk regions are apparently under the two phase conditions. In the innermost bulk region, we can expect that the kinetics is identical to that of homogeneous phase separation, since the perturbation by the solute depletion does not reach the region yet.

Therefore, the typical microstructure of PFZ should be observed at the transient region for the solute depletion case.

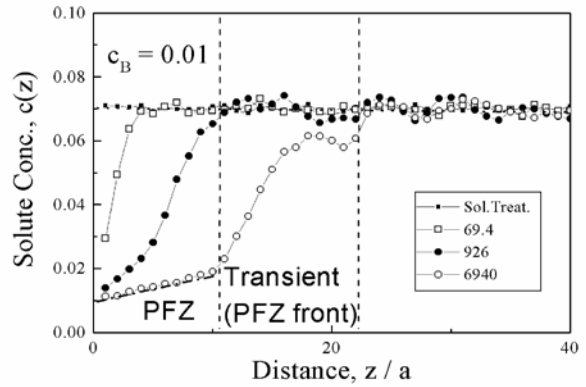

Figure 3: Change in the concentration distribution during aging with the solute depletion at the grain boundary. As described in the previous section, a mass reservoir whose concentration is kept at c_B is attached to the system at z=0. After long time aging, a well defined PFZ and a transient region developed from the grain boundary. z is shown in the unit of lattice constant, a.

The concentration in the transient region changes gradually from the solubility limit to the average composition. This picture naturally suggests that the transient region is the zone that the large precipitates in the bulk region dissolves gradually, and eventually vanishes at PFZ/Transient region interface. On the other hand, many experimental works [3-5] shows that the edge of PFZ is rather clearly observed and no apparent change in average size is seen across the PFZ boundary region. In order to explain this point, the distribution of cluster size around the transient region was examined.

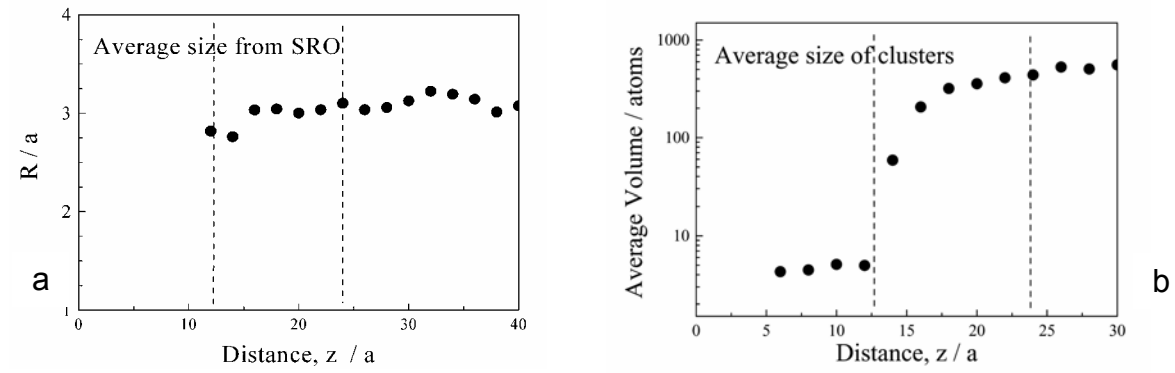

Figure 4: Change in the average cluster size around the transient region. The left (a) figure shows that from average SRO, the size remains almost the same in the transient area, where the SRO is averaged over two

unit cells in z and all the x-y planes. The right (b) figure, in contrast, shows that from the averaging of individual clusters, the average size is decreasing near the PFZ edge.

Figure 4 shows the average size distribution in the PFZ and transient regions, calculated by two different methods described before. From the x-y sectioned averaging as shown in Figure. 4(a), the size is almost constant in the transient region, which agrees with the reported experimental observations.

Although the individual analysis in Figure. 4(b) seem to be different from Figure, 4(a), the difference is explained by the fact that individual counting of the clusters are plotted as a function of their center of gravity, so that considering the size of precipitates itself, Figure. 4(a) and (b) gives the same microstructure.

One interesting point that comes out when comparing the two figures is that, the width of the transient region is of the order of the interparticle distance for the largest part of the size distribution, and the center of gravity for larger particle stays further from the PFZ/transient zone boundary.

This result is understood that the transient region is the zone where the diffusion field made by the grain boundary precipitation is screened by the diffusion field of the precipitates, so that no dissolution of precipitates occurs in the inner part of the sample. This situation is depicted schematically in Figure.5.

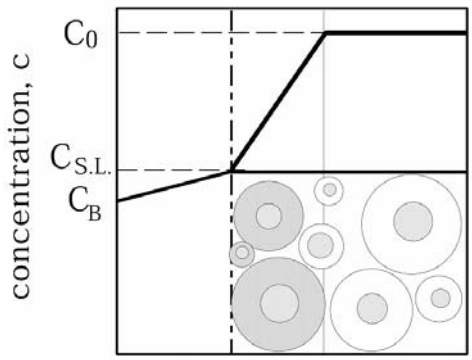

Figure 5: Schematic drawing of the microstructure development in the PFZ and transient region. The precipitates whose diffusion field contact the PFZ region start to shrink. The diffusion fields of precipitates which start shrinking were shown by dark gray circles. C_0, $C_{S.L.}$, and C_B are the average sample concentration, the solubility limit in the bulk at the aging temperature, and the solute concentration at the grain boundary respectively.

3.2 Vacancy Depletion Case

For the vacancy depletion case, the mobility of atoms monotonically decreases near the grain boundary. This picture suggests that the microstructure in the direction normal to the grain boundary looks like isothermal transformation diagram, with the microstructure near the grain boundary corresponding to the initial stage and the structure further into the interior of the grain corresponding to the late stage of precipitation.

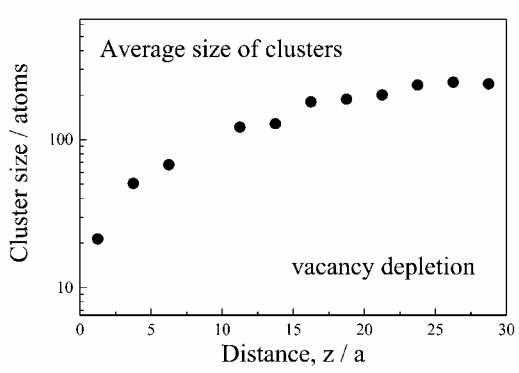

Figure 6: Size distribution in the late stage of aging with vacancy depletion case. It is clearly seen that the average size changes smoothly from the grain boundary to the bulk region.

When the aging treatment at 0.55 Tc was made under the condition that the vacancy concentration profile is expressed by an error function:

$$c_v = c_v^e + (c_v^B - c_v^e) erf(x/2\sqrt{Dt}) \quad (5)$$

with $\xi = \sqrt{Dt} = 180$ unit cells.

Since the vacancy depletion occurs during cooling, with much larger diffusivity at higher temperature, this profile was kept constant during aging, whose characteristic diffusion length remained much smaller.

The resulting distribution of cluster size is shown in Figure. 6. It is clearly seen that the average size of the precipitates increases continuously from the grain boundary to the bulk region. This suggests that in the deep quench condition, we can not find a well-defined PFZ during aging. Although a PFZ might appear in the shallow quench condition, where the incubation in the precipitation process lead to a PFZ, present simulation suggests that no well-defined PFZ should be observed for a aging condition, where no clear incubation appears in the isothermal aging process.

Another important point is that the average size at each position in Figure.6 increases with time, suggesting that PFZ becomes less visible with aging time for single step aging.

4. Conclusions

A Monte Carlo simulation with semi grand canonical boundary conditions at grain boundary and a position-dependent mobility has been used to examine the microstructural characteristics and the kinetics of PFZ formation. When the effect of solute depletion is dominant, a well defined parabolic growth law of PFZ region was observed, with also parabolic growth law for grain boundary precipitates. The size distribution is almost uniform from inside the grain up to the PFZ boundary. On the other hand, vacancy depletion leads to a microstructure whose average size changes continuously. In contrast to the solute depletion case where the PFZ grows with parabolic law, the retarded growth region in the vacancy depletion shrinks with time, and may become less problem in the late aging stage, in particular, under the artificial aging treatment.

Acknowledgement

Part of the present work has been supported by the Nanotechnology metal project of NEDO (New Energy Development Organization), and Light Metals Foundation, Japan.

References

[1] A.K.Vasudevan and R.D.Doherthy, Act Metall. 35(1987)1193.
[2] J.L.Taylor, J.Inst. Metals 92.(1963-1964),301.
[3] P.N.T.Unwin, G.W.Lorimer and R.B.Nicholson, Acta Metall, 17(1969)1363.
[4] J.D.Embury and R.B.Nicholson, Acta Metall, 13(1965)403.
[5] C-H. Joh, K. Yamada and Y. Miura, Mater. Sci. Forum 331-337(2000)1037.
[6] K.Kawasaki. Phys. Rev. 145(1966),224.
[7] J.Gunton and K.Bortz in *Phase Transition and Critical Phenomena*, vol.8, ed Domb and Green, Academic Press, N.Y., 1983.
[8] K.Binder and D.Stauffer, Adv. Collid. Surf. Sci. 10(1979),
[9] B.E.Warren, X-ray diffraction, Dover, N.Y. 1969.
[10] Small-angle scattering of X-rays, Ed. O.Glatter and O.Kratky, Academic Press. NY.1983.
[11] H.Okuda and S.Ochiai, Mater. Trans. in press.